Effect of Inlet/Outlet Fillets on the Clearance Flow in a Rotor-Casing Assembly

Bassam Abu-Hijleh, Jiyuan Tu, Aleksander Subic, and Leigh Fostineo

School of Aerospace, Mech. and Manufacturing Engineering, RMIT University, Victoria, Australia.

Abstract: The performance of a Rotor-Casing Assembly is influenced more by the internal air clearance/leakage paths than by any other thermo-fluid aspect of its behavior. The pressure difference drives the air across the different clearance paths at a rate that is not the same for every path. So the distribution of clearance flow through the various clearance paths within the machine is important for the improvement of the performance. The numerical analysis was conducted using the FLUENT Computational Fluid Dynamics (CFD) package. Geometry definition, mesh generation, boundary and flow conditions, and solver parameters have all been investigated as the part of the numerical analysis. This analysis was conducted for static 2D rotors. Several configurations of inlet only fillets, outlet only fillets, and combined inlet/outlet fillets were investigated. The effects of the fillets on the total clearance flow rate, distribution of the flow among the different paths, and the turbulent kinetic energy within the rotor-casing assembly are reported and discussed. In general, the use of outlet only fillets had little effect on the flow field. The use of small fillets (2 mm) on both inlet and exit provided significant reduction in the turbulent kinetic energy indicating improved system efficiency.

Keywords: *Supercharger, Clearance flow, Leakage, CFD, Numerical.*

1. INTRODUCTION

Environmental issues have been highlighted in recent years on a global level, and motor vehicles are required to meet severe requirements for fuel consumption and exhaust gas control while satisfying various driving requirement of the users. To meet these requirements, motor engines equipped with high-response superchargers are being introduced to the market (Yoshiyuki et al., 2001). The Twin Screw Supercharger (TSSC) is a positive displacement compressor, the working cavity of which is enclosed by the casing bores, casing end plates and the helical surfaces of the male and female rotors. As the rotors rotate, the volume of the working cavity varies from zero to its maximum and from its maximum to zero periodically in a manner determined uniquely by the geometry of the supercharger. As a consequence of this periodic variation, the supercharger completes its suction, compression and discharge processes.

This paper demonstrates a two-dimensional model of a supercharger. Due to the geometry of the rotor-casing assembly, the clearances between two rotors and the clearances between rotors and casing, air clearance flow paths exist within the supercharger assembly. The internal flow rate is dependent on three different clearances: between the casing and male rotor (C-M), between the two rotors (M-F), and between the female rotor and the casing (F-C) (Takei and Takabe, 1997; Flemin and Tang, 1995). It is very important to know the total clearance flow rate as well as the distribution of the flow among each clearance path for the purpose of design procedures in general and for improving the rotor lobe profile.

CFD analysis is performed using the FLUENT CFD package, which is employed to simulate the flow passage through the supercharger. The flow is simulated as a steady 2-D turbulent incompressible air using the Realizable k-ε turbulence model. The Realizable k-ε turbulence model is employed because it has shown substantial improvements over the standard k-ε model where the flow features include strong streamline curvature, vortices, and rotation (Shih et al., 1995).

2. COMPUTATIONAL TECHNIQUE

The 2-D geometric model is produced from the AutoCAD engineering drawings of the Sprintex supercharger. This supercharger assembly consists of a male rotor, a female rotor and a casing. Clearances are formed between the two rotors, and between the rotors and casing. Figure (1) shows the "reference" position, when the two rotors are fully meshed. The placement of the inlet (I) / outlet (O) fillets can also be seen in Figure (1). The distance between the centres of the two rotors is 65.8 mm, resulting in a nominal clearance of 0.2 mm. The clearance between the rotors and the casing is also 0.2 mm. Two other rotor positions are also included in this study: the "start" position, when the two rotors start to mesh, and the "end" position, when the two rotors begin to move apart after completing the meshing process, Figure (2). In modelling the inlet and outlet as a pressure boundary condition, their locations are placed far enough in order not to affect the flow in the casing.

The pre-processor used in this investigation, GAMBIT, imports the geometry files and generates the flow domain. A tri-elements grid is applied to the domain. A boundary layer of elements is created along the walls and the tips of the rotors to accurately simulate the high velocity

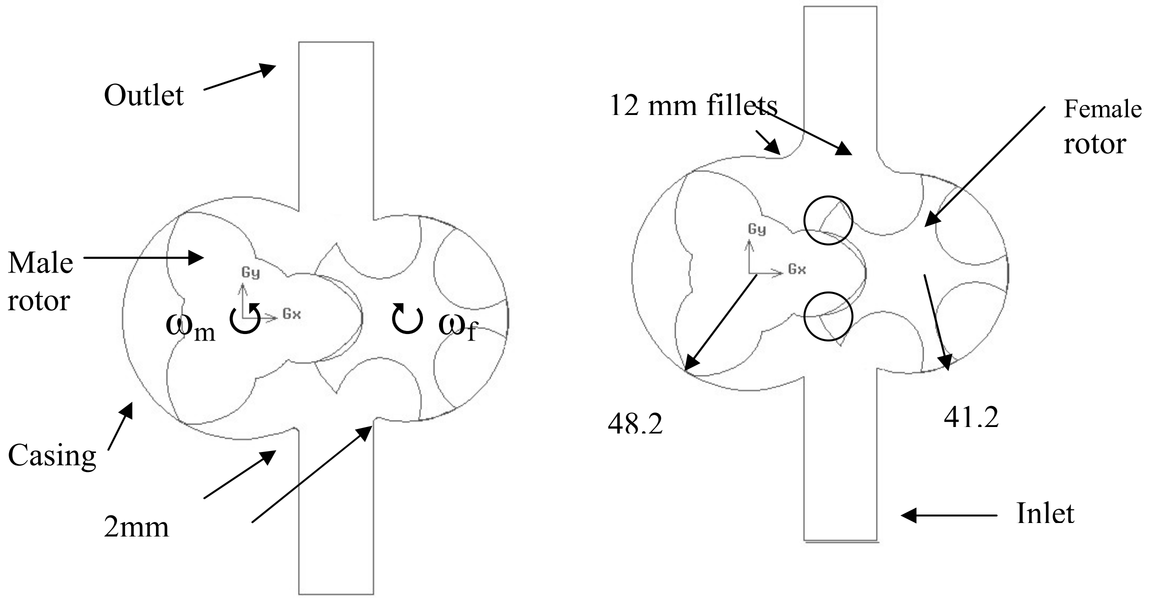

Figure 1. A schematic of the supercharger assembly in the "reference" position showing an inlet fillet only of 2mm (left) and an exit fillet only of 12mm (right).

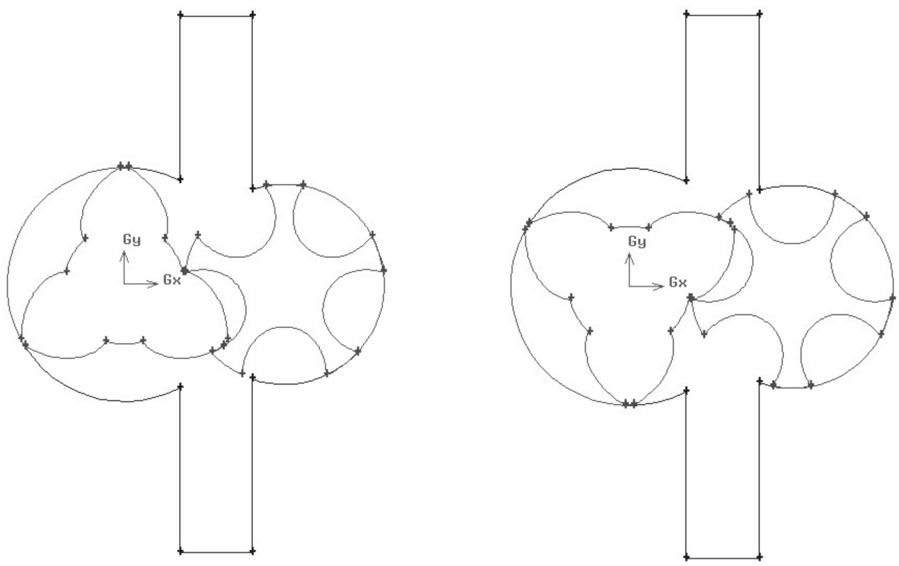

Figure 2. A schematic of the supercharger assembly showing the "start" (left) and "end" (right) positions. There are no fillets on these two configurations.

gradients at these locations. The grid used was sufficiently fine to insure at least five elements in the narrowest passage between the two rotors. The grid sizes used ranged between 200,000 – 250,000 elements, depending on the radius of the fillet(s) used. Grid refinement tests indicated that the solutions obtained using such grids to be grid independent. The residual convergence value used is 1E-4. Smaller residual values did not result in any noticeable change of the calculated results but required significantly more computation time.

3. RESULTS

Figure (3) shows the change in the total clearance flow rate as well as its breakdown between the three clearance paths as a function of the pressure ratio (PR) between the inlet and exit. The results in Figure (3) are for the rotors at the "reference" position. As expected all clearance flow rates increase with pressure ratio, but not in a linear fashion. The reason for that is that as the pressure ratio increases the air speed in the different clearance passages increases considerably. The friction losses are proportional to the square of the speed thus the non-linear behaviour in Figure (3).

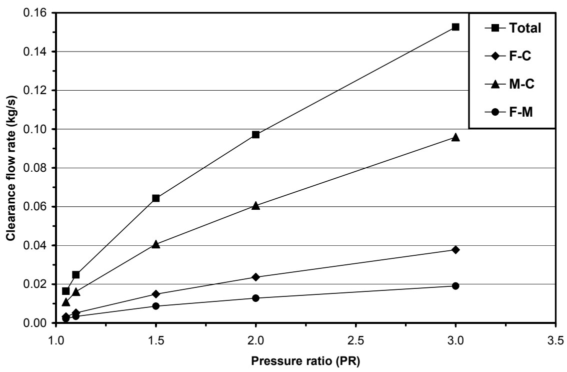

Figure 3. Clearance flow rate as a function of pressure ratio. Rotors at "reference" position.

The major clearance flow is between the male rotor and the casing (M-C) followed by that between the female rotor and the casing (F-C) and lastly between the female and male rotors (F-M). The cause of this can be traced to the flow resistance of each path, which is proportional to the length and width of each path. From Figure (1) we can see that the total length of the three clearance paths between the female and the casing is much bigger than the total length of the two clearance paths between the male and the casing. Thus less air will flow between the female rotor and the casing (F-C) than between the male rotor and the casing (M-C). As for the path between the two rotors (F-M), there are two pinch points at the top and bottom of the meshed portions of the rotors, highlighted by the circles in Figures (1). The clearance between the two rotors at these pinch points is much less than the clearance between the rotors and the casing, 0.08 mm vs. 0.2 mm. Thus the high flow resistance between the two rotors, which results in the lowest flow of the three clearance paths. The overall trend in flow distribution between the three clearance paths does not change with pressure ratio. Thus a single pressure ratio, PR=2, will be used for the reminder of this work.

The absolute and relative changes in the clearance flow as a function of the rotors' meshing positions can be seen in Figures (4 and 5), respectively. The results in the two figures are for a pressure ratio (PR) of 2. The "start" and "end" positions have a lower flow rate than the "reference" position, Figure (4). This is mainly due to the much smaller pinch clearance between the two rotors at these positions, Figure (2). Figure (5) shows that the relative distribution of the leakage between the three leakage paths remains almost constant. The only noticed change is the reduction in the (F-M) leakage at the "start" and "end" positions as compared to the "reference" position. This is due to the reduce pinch clearance as discussed above. Based on these results, the effect of inlet (I) and outlet (O) fillets will be investigated only for the "reference" position.

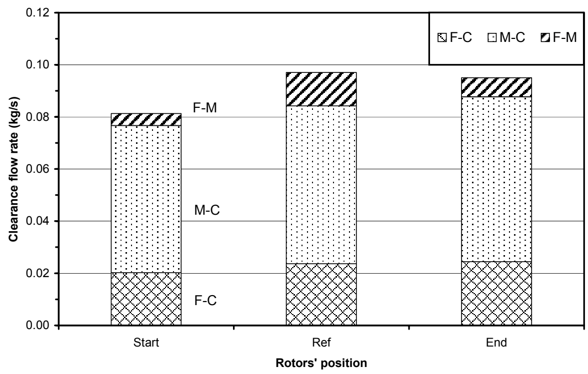

Figure 4. Magnitude & distribution of the clearance flow at the three rotors positions, PR=2.

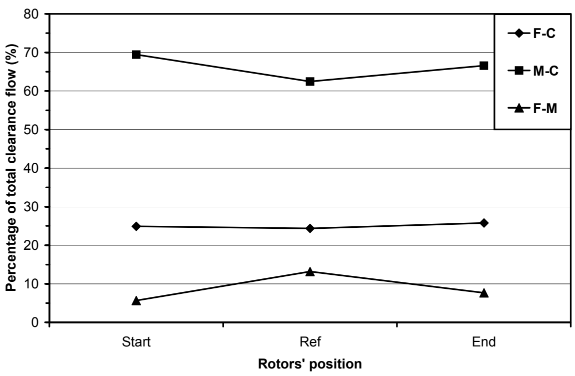

Figure 5. Relative distribution of the clearance flow at the three rotors positions, PR=2.

Figure (6) shows the changes in the clearance flow rate as a function of different inlet and outlet fillet configurations. The figure includes an extra configuration (I=1 mm & E=1 mm), which was intended to see the lower limit on the fillet size that can be used. Using fillets on the exit only did not seem to have a significant effect the clearance flow rate, Figure (6). Using fillets on the inlet only was more significant and resulted in up to 3.5% change in the clearance flow. With exit fillets having minimum effect on the clearance flow rate, one would expect that the results of using inlet and exit fillets would be similar to those of inlet only fillets. This was not the case, as shown in Figure (6). The use of small fillets (≤ 4 mm) on both inlet and exit resulted in a slight reduction in the clearance flow. For larger fillet radii (> 4 mm), the clearance flow rate increased but remained less than that of the inlet only fillets cases.

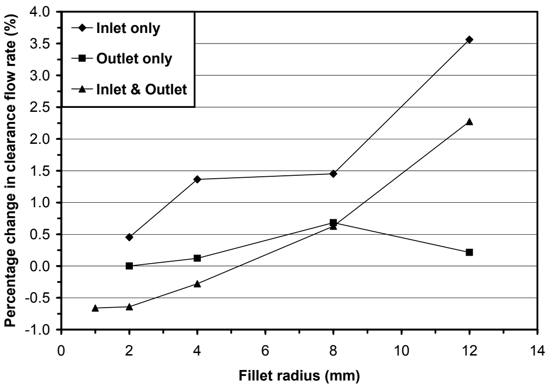

Figure 6. Percentage change in the clearance flow rate as a function of inlet/exit fillets. PR=2 and rotors at "reference" position.

Figure (7) shows the changes in the maximum turbulent kinetic energy as a function of different inlet and outlet fillet configurations. The use of inlet only or exit only fillets seems to have a similar effect on the maximum turbulent kinetic energy. Both configurations reduce the maximum turbulent kinetic by about 10-15%. Furthermore, the changes in the maximum turbulent kinetic seem to be almost constant with little dependence on the fillet radius. Small fillets reduce the regions of high turbulence compared to the no fillets configuration, thus the reduction seen in Figure (7). But as the fillet radius increases, the fillets give rise to new regions of high turbulence, thus the trend seen in Figure (7). The fillet size of 2 mm seems to be the best. Figure (8) shows the turbulence contours of different inlet (I) and exit (E) fillet configurations. All counters have a common scale, shown next to the no fillet configuration (I=0 & E=0). The superiority of using small fillets ant inlet and exit is clear.

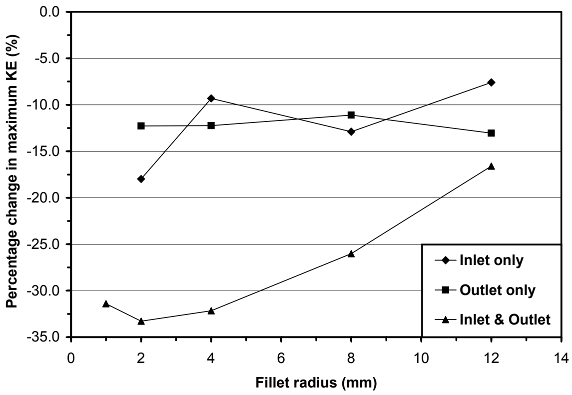

Figure 7. Percentage change in the maximum turbulent kinetic energy as a function of inlet/exit fillets. PR=2 and rotors at "reference" position.

4. CONCLUSIONS

The clearance flow rate is non-linearly proportional to the pressure ratio across the rotor-casing assembly. Most of the flow goes through the M-C path followed by the F-C and F-M paths, respectively. The magnitude and distribution of the clearance flow does not change much with rotor position. The use of fillets can increase or decrease the clearance flow rate but always reduce the maximum turbulent kinetic energy. The best fillet combination seems to be I=2 mm & E=2mm. The reduction in turbulent kinetic energy should translate into lower energy losses within the rotor-casing assembly and thus a more efficient system.

5. REFERENCES

Fleming, J.S. and Tang, Y. Analysis of leakage in a twin screw compressor and its application to performance improvement, *Journal of Process Mechanical Engineering*, 209, 125-136, 1995.

Shih, T. -H., Liou, W. W., Shabbir, A. and Zhu, J. A New k-ϵ Eddy-Viscosity Model for High Reynolds Number Turbulent Flows - Model Development and Validation. *Computers & Fluids*, 24(3), 227-238, 1995.

Takei, N. and Takabe, S. Optimization in performance of Lysholm compressor, *JSAE Review*, 18, 331-338, 1997.

Yoshiyuki, M., Kaoru, K., Mitsushi M. and Yoshihito, K. Development of New Automotive Supercharger, *HI Engineering Review*, 34(2), 2001.

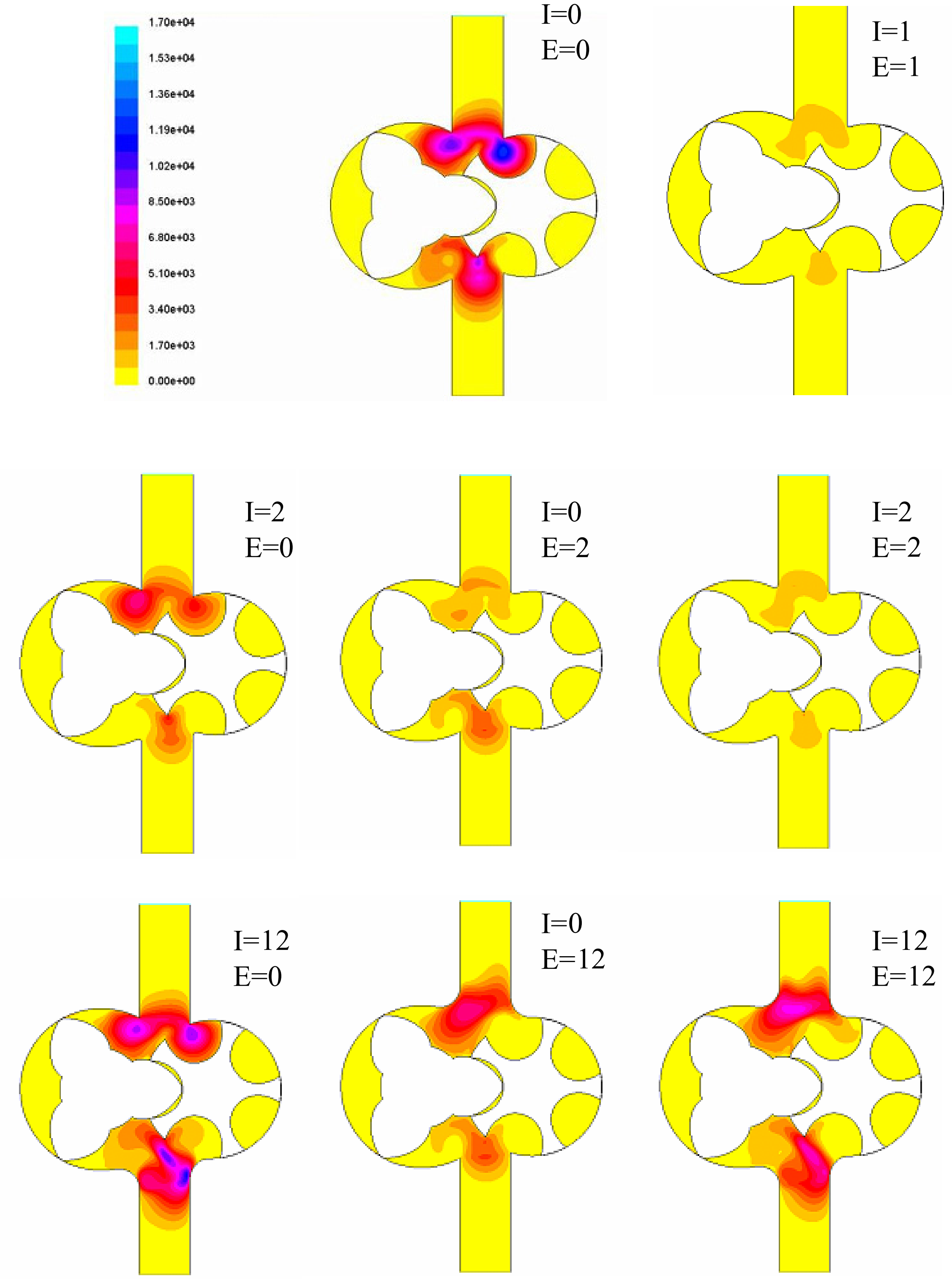

Figure 8. Contours of the turbulent kinetic energy for different inlet/outlet fillet configurations, uniform scale. PR=2 and rotors at "reference" position.